

Blue Delayed Luminescence Emission in Neutral Nitrogen Vacancy Containing Chemical Vapor Deposition Synthetic Diamond

Ffion L. L. James,* Amber M. Wassell, Colin D. McGuinness, Peter M. P. Lanigan, David Fisher, Georgina M. Klemencic, Chris Hodges, and Stephen A. Lynch

Herein, the authors investigate the temperature-dependent properties of delayed luminescence in an as-grown nitrogen-containing chemical vapor deposition synthetic diamond gemstone when excited above its bandgap. At room temperature, this gemstone exhibits delayed luminescence from nitrogen-vacancy centers at 575 nm. However, at 77 K, the first recorded instance of a long-lived delayed blue luminescence centered at ≈ 465 nm, accompanied by spectral peaks at 419, 455, and 499 nm is reported. By analyzing spectral and temporal data at different temperatures, it can be speculated on potential photophysical transitions. This discovery documents the initial observation of this delayed luminescence emission, contributing to the collective understanding of synthetic diamonds.

radiation ($\lambda < 225$ nm) at room temperature. This phenomenon forms the basis for the De Beers SYNTHdetect instrument, which is used to distinguish between natural and synthetic diamonds.^[4] Recently, we have observed a delayed spectrally broad blue luminescence centered at 465 nm in a synthetic diamond grown by chemical vapor deposition (CVD) when measured at temperatures below 190 K. This previously undocumented blue emission, not yet fully understood, serves as a reference point in our exploration of synthetic diamonds. We intend to introduce this novel feature to the scientific community, marking its initial identification as a phenomenon.

1. Introduction

Diamonds have been highly prized and valued as natural gemstones for centuries, and confirming that a diamond is a high-value natural stone rather than laboratory-grown is essential for the maintenance of consumer confidence in today's jewelry market. There are numerous interrogation methods available to gemmologists to screen for synthetic diamond gemstones, particularly optical spectroscopy and imaging.^[1,2] Certain optical signatures are of specific use in positively identifying a natural diamond.^[3] The vast majority of natural type IIa and type Ia colorless diamonds are known to exhibit a delayed luminescence centered at 455 nm when excited with pulsed short-wave UV


2. Experimental Section

An untreated nitrogen-doped CVD diamond from Element Six had its nitrogen concentration determined to be 0.13 ppm using UV absorption techniques. The sample has the characteristics presented in **Table 1**. The sample was subjected to four experiments: 1) temperature-dependent photoluminescence measurements taken concurrently with the initial excitation henceforth referred to as “prompt” photoluminescence; 2) temperature-dependent photoluminescent measurements taken 90 μ s after the initial excitation, henceforth referred to as “delayed” photoluminescence; 3) time-gated imaging; and 4) time-resolved photoluminescence measurements at two specific wavelengths.

Prompt and delayed photoluminescence spectra of the sample were measured as a function of temperature in the range 77–350 K. Sample excitation was provided by a Hamamatsu Photonics L7685 xenon flash lamp, which was spectrally filtered by a bespoke band-pass filter (laser components) used to give a 190–227 nm output with a temporal pulse duration of 2.9 μ s at full-width half maximum. A Horiba iHR-320 spectrometer with a 300 g mm⁻¹ grating was used with an Andor iStar DH320T-18U-E3 intensified charged-coupled device (iCCD) camera to record the spectral data. A pulse generator was used to provide two externally generated transistor–transistor–logic signals for the synchronization of the camera and flash lamp. To overcome the electrical signal latency recorded between the camera and the flash lamp, the internal timer of the camera was used to offset the flash lamp's signal by 8 μ s. To record the prompt luminescence, the iCCD delay was set to zero to allow the emission to be

F. L. L. James, A. M. Wassell, G. M. Klemencic, C. Hodges, S. A. Lynch
School of Physics and Astronomy
Cardiff University
Cardiff CF10 3AT, Wales, UK
E-mail: Jamesf11@cardiff.ac.uk

C. D. McGuinness, P. M. P. Lanigan, D. Fisher
De Beers Ignite
Belmont Road, Maidenhead, SL6 6JW Berkshire, UK

 The ORCID identification number(s) for the author(s) of this article can be found under <https://doi.org/10.1002/pssa.202300651>.

© 2024 The Authors. physica status solidi (a) applications and materials science published by Wiley-VCH GmbH. This is an open access article under the terms of the Creative Commons Attribution License, which permits use, distribution and reproduction in any medium, provided the original work is properly cited.

DOI: 10.1002/pssa.202300651

Table 1. Sample characteristics of the CVD nitrogen-doped diamond.

| Diamond type | Weight | Impurity level | Shape and cut | Color grade | Clarity grade |
|--------------|--------|----------------------|-----------------|-------------|---------------|
| CVD | 0.4 Ct | 0.13 ppm of nitrogen | Round brilliant | L | VS1 |

detected during the firing of the lamp pulse. A delay of 100 μ s was set before the emission signal of the delayed luminescence was recorded. This emission was integrated over a 30 ms gate and accumulated 20 images.

Time-gated imaging of the sample's luminescence was collected via a Basler Ace acA1920-40uc area scan camera. For prompt luminescence measurements, a temporal offset of 11 μ s was introduced between the camera and the flash lamp for the data collection to overcome the time delay noted when both devices were electrically triggered simultaneously.

Time-resolved delayed luminescence measurements of the sample were taken using a thermally cooled Horiba Jobin Yvon IBH TBX-04 photomultiplier via a Horiba iHR-320 spectrometer. The detector and flash lamp were triggered simultaneously, with channels recording both the prompt and delayed luminescence in each time sweep of the multichannel analyzer. The time spacing of the channels was selected to suit the decay time being measured. After the data were accumulated, the channels recording prompt luminescence were rejected.

3. Results

The prompt and delayed temperature-dependent photoluminescence spectra are shown in **Figure 1**. In **Figure 1a**, the presence of a neutral nitrogen-vacancy (NV^0) defect is evident, identified by its characteristic zero-phonon line (ZPL) at 575 nm.^[5] The intensity and sharpness of this ZPL peak are at their lowest at 350 K but increase as the temperature decreases.^[6]

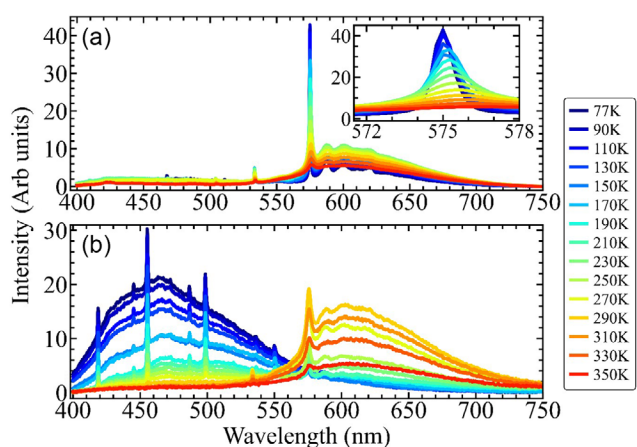


Figure 1. Photoluminescence spectra measured at temperatures in the range 77–350 K for a 0.13 ppm nitrogen-doped single crystal CVD diamond. a) The prompt photoluminescence is measured concurrently with the initial excitation, with an insert highlighting the NV^0 center at 575 nm. b) The delayed photoluminescence is measured at 90 μ s after initial excitation. Emission from the NV^0 center at 575 nm is highlighted for both prompt and delayed photoluminescent spectra.

Similar temperature-dependent behavior is observed for another peak at 535 nm, though the defect responsible for this peak remains unidentified.^[7,8]

Figure 1b shows the temperature dependence of the delayed photoluminescence measured at 90 μ s after initial excitation. The intensity of the NV^0 center photoemission located at 575 nm and the smaller spectral peak at 535 nm increase at 290 K, with observed diminishing intensity and sharpness as the temperature increases above this. As the temperature is reduced, a previously undocumented broadband emission feature centered around 465 nm appears with 3 distinct protruding peaks at 419, 455, and 499 nm. The highest intensity for both the three peaks and the broadband emission feature was measured at the lowest temperature (77 K). Below 190 K, three additional smaller peaks emerge on the broadband emission feature at 445, 489, and 550 nm, and increase in intensity as the broadband emission feature grows with decreasing temperature.

Interestingly, as the temperature is reduced below 290 K, both the 575 and 535 nm peaks show a gradual decrease in recorded intensity until they are hidden by the broadband emission feature at 77 K.

Figure 2 shows the amplitudes of the delayed luminescence peaks observed at specific wavelength positions: 465 nm (position within the broad blue spectral feature from **Figure 1b**), 419, 455, and 499 nm (representing the sharp peaks observed atop the broadband emission feature from **Figure 1b**), 575 nm (ZPL NV^0), and 737 nm (ZPL SiV^-). The excitation and collection parameters remained constant for successive temperature-dependent measurements when these amplitudes were taken.

We have included the intensity response of the 737 nm SiV^- center in **Figure 2** for completeness to show the absence of SiV^-

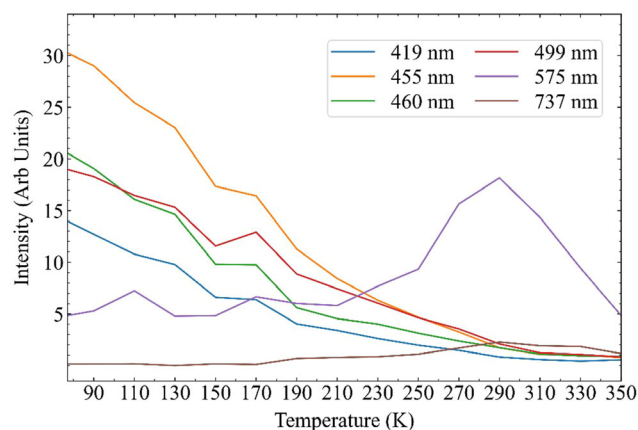


Figure 2. Intensity of the 90 μ s delayed luminescent peaks observed at specific wavelength positions from **Figure 1b**: 465 nm (position within the broadband feature), 419, 455, and 499 nm (positions of the sharp peaks observed atop the broadband feature), 575 nm (ZPL NV^0), and 737 nm (ZPL SiV^-).

centers within our sample, as there is no discernible SiV^- peak in either Figure 1b or 2, as if the SiV^- center was present, we would expect a distinct peak similar to that shown in ref. [5]. The slight increase observed at the 737 nm wavelength in Figure 2 is more likely attributed to the broad trail associated with the increasing NV^0 center rather than being a signal from the SiV^- ; if any signal is present, it is likely obscured by background noise.

The intensity recorded at 575 nm has an increasing intensity to a maximum of 290 K and decreases thereafter as the temperature is increased. The opposite response is noted for the amplitudes at 435, 455, 465, and 499 nm as they exhibit decreasing intensity as temperature rises.

A visual inspection of the emission from the sample was undertaken using time-gated imaging for a range of temperatures (77, 150, and 296 K) and time delays after initial excitation before capturing an image (0, 90 μs , and 70 ms). Each image was taken with an integration time of 30 ms. The time-gated images are shown in Figure 3.

For measurements at 296 K (bottom row), a decrease in intensity and a blue/red shift in color is observed as a function of increasing delay time from 0 to 70 ms. There is an observable color shift as the emission spectrum changes, transitioning from yellow/gold to orange until no detectable emission is observed. At a reduced temperature of 150 K (middle row), the evolution of the emission color as a function of delay time is markedly different. As the delay time is increased, the emission changes from pale yellow to turquoise, to blue with a concurrent decrease in intensity. Similar behavior is observed as the temperature is further reduced to 77 K (top row), except that the transition from yellow to blue happens sooner and the intensity takes longer to decrease, with an appreciable intensity remaining at 70 ms.

An alternative interpretation of Figure 3 is to consider the effect of varying temperatures at a fixed delay time. At 0 μs delay (left column), the intensity of the emission increases as the temperature is reduced; at the lowest recorded temperature, a slight

blue tinge is observed, indicating a small amount of blue emission. After a delay of 90 μs (middle column), there is a significant difference in the color of emission as a function of temperature varying from orange at the highest temperature, to turquoise, to blue at the lowest temperature. The turquoise emission observed at 150 K also appears to be brighter than its counterparts for a 90 μs delay. At a 70 ms delay (as indicated in the right column), the camera barely captured an extremely faint emission at 296 K. As the temperature is reduced, a blue emission is observed with a higher intensity at the lowest temperature.

The observed transition from a blue to an orange emission with increasing temperature is illustrated in Figure 3. This transition is in agreement with the spectral data presented in Figure 1b and 2. Figure 1b demonstrates that as the recorded temperature increases, the spectral data associated with the blue emission (left-hand side of Figure 1b) exhibit a decrease in intensity, ultimately giving way to the emerging orange emission (right-hand side of Figure 1b) associated with the NV^0 center. Both Figure 1b and 2 highlight that the NV^0 center emission is most prominent in the delayed luminescence timescale at 290 K, which justifies its selection for comparison with other temperatures in Figure 3.

Finally, time-resolved decay measurements were made of the sample emission in the temperature range 77–350 K at 575 and 455 nm. These wavelengths were chosen due to their association with the NV^0 defect (575 nm) and the identification of the sharp peak with the highest intensity within the range of the broadband emission feature centered at 465 nm (455 nm). Figure 4 shows the temperature-dependent decay emission at 455 (Figure 4a) and 575 nm (Figure 4b); these observed decay measurements include a contribution from the underlying broader blue emission. The first 330 channels (containing photons) were removed by the Horiba Fluorescence Decay Analysis Software (DAS6). These photons were removed: 1) before the maximum photon intensity was reached (before excitation); and 2) immediately after excitation to compensate for detector saturation from the prompt luminescence of the sample.

The decay data for both wavelengths cannot be adequately described by a single exponential, which would be characteristic of a simple population decay model. A better fit is produced using 3 or 4 exponentials (solid lines in Figure 4), suggesting that there are multiple decay processes happening simultaneously.

Each decay process has its own lifetime, making the transient convoluted and challenging to interpret. For the emission at 455 nm, a short lifetime component develops as the temperature increases from 77 to about 150 K, but is absent above this with an additional short lifetime component emerging at 310 K. The NV^0 emission also shows a significant short lifetime component, but this is only present at 250 K and above.

Due to the complexity of the decay data, a clear understanding of the relaxation processes within the sample would require deconvolution of the data, with individual analysis of each transient component. However, to gain some initial understanding of the decay process occurring within the unknown blue center within the sample, we calculated the average decay lifetime for each temperature using a weighting of the sum of the pre-exponentials needed to describe the data, acknowledging the limitations of this method since it lumps together several decay transients. Nevertheless, this analysis serves as a straightforward

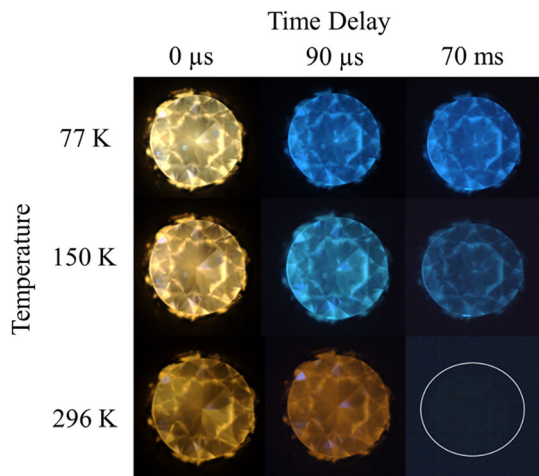


Figure 3. Time-gated images of the nitrogen-doped sample as a function of temperature and delay after initial excitation. The images were recorded at 77 (top row), 150 (middle row), and 296 (bottom row) with a delay of 0 s (left column), 90 μs (middle column), and 70 ms (right column). At 296 K, there is an absence of measurable emission after a delay of 70 ms; the white circle (bottom right) indicates the sample location.

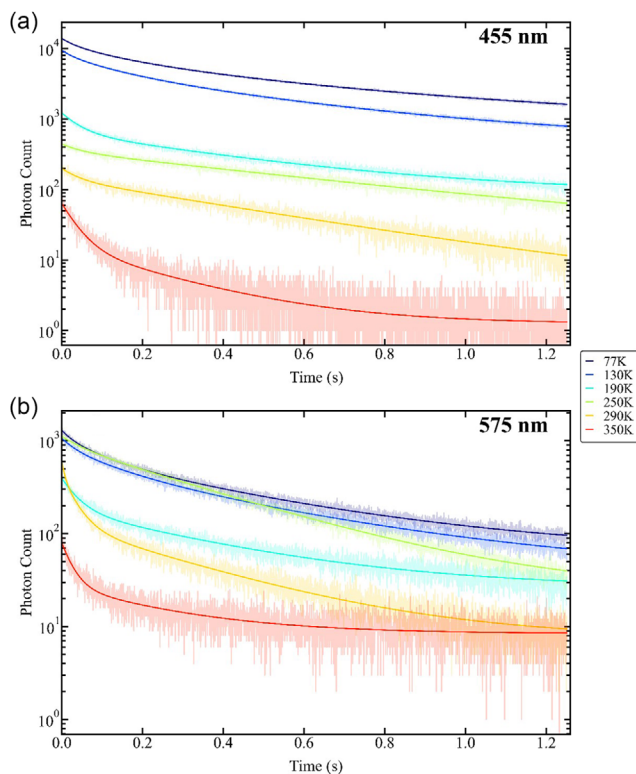


Figure 4. a) Decay of the sample emission at 455 nm and b) at 575 nm for temperatures in the range of 77–350 K. The solid lines are a multiexponential fit consisting of either 3 or 4 exponentials.

way to quantify the decay time while being mindful that the data do not follow the single exponential characteristic of a simple population decay model.

Figure 5 shows the calculated time-resolved decay lifetimes (τ) for spectral emissions centered at 455 (blue) and 575 nm (orange). For 455 nm, average decay lifetimes were calculated using either three or four exponential decays, while for 575 nm a fit using only three exponentials was sufficient to describe the data. The average decay lifetimes calculated for 455 nm decrease linearly from 0.26 to 0.14 s over the temperature range 77–190 K

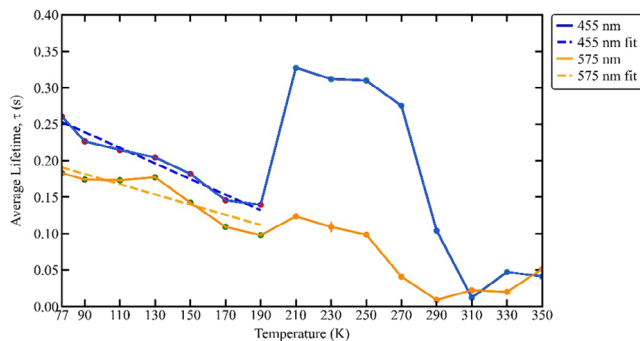


Figure 5. Decay lifetimes (τ) of the sample emission at 455 (blue) and 575 nm (orange) for temperatures 77–350 K. The blue and orange dashed lines are guides to the eye for $\tau(T)$ over a temperature range of 77–190 K, with points of interest colored red for 455 nm and green for 575 nm. If not visible, error bars fall within the marker size.

before a rapid increase to 0.33 s is observed at 210 K. This longer average lifetime plateaus between 210 and 250 K before the average lifetime drops to its lowest point at 310 K.

The calculated decay lifetimes for emission centered at 575 nm show a very similar linear decrease as the temperature increases to 190 K, but the large increase and plateau seen for 455 nm is absent and is replaced with a moderate lifetime increase which settles back down at 270 K.

4. Discussion

To understand the sample’s photoluminescence behavior with respect to temperature, both the prompt (at the time of initial excitation) and the delayed (90 μ s after initial excitation) luminescence response were considered. The prompt luminescence spectra in Figure 1a show emission from the NV⁰ center.^[6]

Figure 1a also highlights that as the temperature increases, the recorded ZPL response changes; using a Lorentzian function, we can note that the line widths broaden and the intensity decreases. Equation (1) expresses the inverse relationship between the width (Γ) of a Lorentzian fit and the lifetime (τ) of the associated process, highlighting the broadening of the ZPL as the NV⁰ center’s lifetime decreases. This method can be used as an indication of the upper limit of the decay lifetime of the NV⁰ center at these temperatures (from 77 to 350 K). With the shortening lifetime of the NV⁰ center, it may be hypothesized that during the higher temperatures, the NV⁰ center has a limited duration of existence before undergoing a transformation or decay implying the nitrogen and vacancies assume a more energetically favorable form.^[7]

$$\Gamma = 1/\tau \quad (1)$$

As temperature increases, a slight redshift is observed. For instance, at 77 K, the peak is centered at 575.0 nm, whereas at 350 K, the peak is centered at 576.3 nm. Dong et al.^[8] attributed a shift in defect energy levels as a result of increasing thermal lattice expansion and phonon interactions within the lattice.^[9]

Additionally, the width of each peak, as recorded for different temperatures, also increases with rising temperatures. Specifically, the width changes from 0.46 nm at 77 K to 3.51 nm at 350 K.

Figure 1a also highlights the small peak recorded at 535 nm; this has been tentatively described as a nitrogen-containing cluster defect in CVD-grown diamond by Zaitsev et al.^[10] as a CVD-related signal in the literature.

The sample’s delayed luminescence spectra shown in Figure 1b shows the appearance of both the previously unknown broadband emission feature of unknown origin centered at \approx 465 nm with three distinct peaks at 419, 455, and 499 nm which appear as the temperature is decreased below 210 K, in addition to a peak at 575 nm.

On these delayed timescales, the intensities of the recorded 575 nm peak are much lower, with the highest intensity of the 575 nm peak measured at 290 K instead of at 77 K, as seen in the prompt luminescence spectra shown in Figure 1a. The overall lower intensity recorded at 575 nm is to be expected due to a partial decay occurring before the recording commenced 90 μ s after the initial excitation.

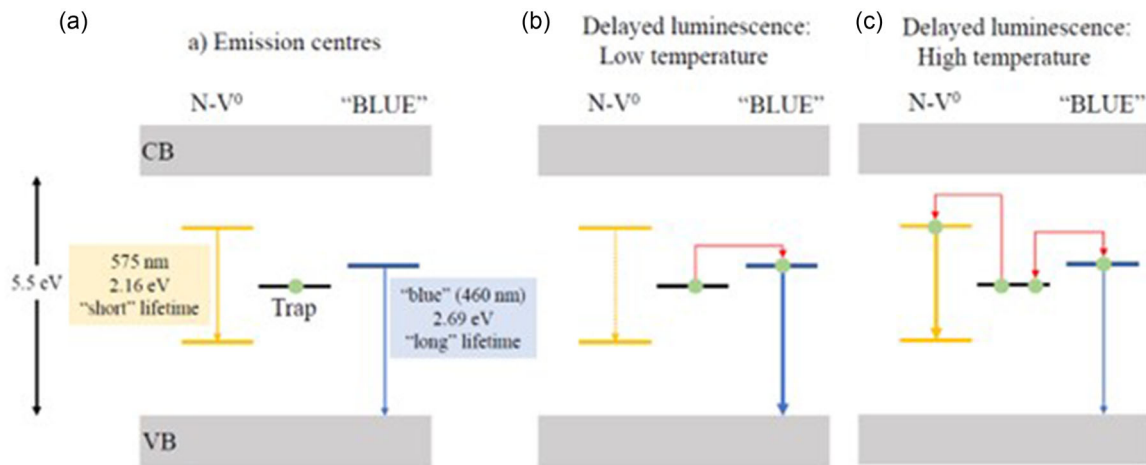


Figure 6. Speculated energy levels within the sample: a) the proposed emission centres including the known NV^0 , a proposed trap state (“Trap”), and an unknown “blue” center (“Blue”). b) Proposes the transition on the delayed luminescence timescale at low temperatures; electrons leave the trap state and decay through the blue state. c) Proposes the transitions that occur on the delayed luminescence timescale at high temperatures; electrons transition to the favored blue center before some of the electrons jump back to the trap state and subsequently decay through the NV^0 center due to the extended lifetime of the blue center, similar to prompt emission behavior.

In **Figure 6**, we postulate a preliminary energy level diagram aimed at elucidating the immediate luminescence and the temperature-dependent delayed luminescence. The main aspects of this proposed diagram are as follows: 1) it includes a trap state positioned slightly below the excited states of NV^0 and blue centers, with the NV^0 excited state just above that of the blue center; and 2) it assumes that the charge carriers have already reached thermal equilibrium with the bottom of the band. It is worth noting that this simplified model explores a scenario occurring over a significantly longer timescale compared to the timescale associated with charge carriers rapidly reaching the bottom of the band. We acknowledge the distinct spectral peaks (Figure 1b) within the 400 to 550 nm range, likely corresponding to discrete energy levels and potential excited states inside the defect center. However, we refrain from including speculative internal energy levels to avoid overcomplicating the discussion with details unsupported by our current data. NV^0 emission dominates the prompt luminescence which is consistent with its shorter lifetime and possibly a higher capture probability for excited electrons. Delayed luminescence could be produced via the de-excitation of electrons thermally scattered from the trap center and subsequently captured by either the NV^0 or the blue centers.

As the temperature is increased during the delayed luminescence emission, more electrons may be thermally scattered into the NV^0 center excited state, resulting in the emission from the NV^0 center to strengthen at the expense of the blue emission. The fact that the NV^0 emission eventually becomes dominant is a consequence of its shorter lifetime and higher capture probability, similar to the situation for prompt luminescence. However, at the lowest temperatures, emission from the blue center dominates, suggesting the alternative decay pathway through the NV^0 center has been switched off. Electrons within a system at room temperature are known to possess approximately 25 meV of thermal energy. In light of this observation, we acknowledge that future work could involve far-infrared and terahertz measurements to estimate the energy level of

the trap state relative to NV^0 and the blue state within our sample. These measurements may be able to reveal the presence of the proposed trap state to explore the alternative decay pathways within the diamond energy level landscape. These alternative pathways may open up other avenues of research.

Figure 2 highlights this proposed transition of the dominant center, from the blue to the NV^0 center; however, during this transition, there is a significant drop in the 455 nm emission seen before any corresponding rise in the 575 nm emission. This observation challenges our expectation, where we anticipated that electrons excited from the trap to the blue center would promptly return to the trap and then move to the excited state of the NV^0 center leading to a fast increase in the 575 nm emission as the 455 nm emission decreases. However, there is an observable time delay between the decrease in 455 nm emission and subsequent increase in 575 nm emission suggesting there may be additional dynamics missing in our simplistic schematic, as shown in Figure 6.

The time delay between the noted emission may suggest additional nonradiative decay centers playing a role at low temperatures, potentially perturbing the decay dynamics of the electrons instead of the NV^0 center. The possibility of other radiative decay pathways at low temperatures is supported by the observation of sharp peaks at 419, 455, and 499 nm superimposed on the broad spectral feature at 465 nm. Sharp spectral lines typically indicate discrete energy transitions between distinct levels, while broad spectral features often signify energy transitions from a discrete level into a continuous band, both of which appear at lower temperatures.

The indication of alternative or additional decay pathways other than the NV^0 center in our sample is further supported by the data in Figure 1–3 when the NV^0 center no longer has a spectral emission and an unidentified entity (blue center) begins to emit a spectral emission as the temperature decreases. The proposed transition from an NV^0 center to an alternative center is further supported by the color change, as shown in Figure 3. The associated color of an NV^0 center (yellow/gold)^[11]

is observed to transition to a blue emission as the temperature is decreased and the time delay between excitation on imaging of the stone is increased. Our investigations into the mechanism behind this blue emission center have prompted further questions since the newly observed sharp emission peaks at 419, 455, and 499 nm could indicate further discrete energy levels within the bandgap. It is important to note, however, that our understanding is still limited, and further research is required to fully comprehend the nature and potential of this blue center.

Lifetime decay studies were also performed for the emission at 455 and 575 nm, as shown in Figure 4, which highlights that the decay has a temperature dependence. Figure 4a shows that the intensity of the decay time signal recorded at 455 nm increases as the temperature decreases. The optical signature of our suggested unknown impurity complex is not observed at higher temperatures though attains its longest lifetime at 77 K—the lowest temperature accessible in our experiment setup. As the temperature increases, the gradual decrease in decay time implies a corresponding transformation is occurring between this unknown complex and the previously recorded NV⁰ defect.

In Figure 5, we display the average decay lifetime, τ , as a function of temperature. The decay lifetime represents a time constant that characterizes the speed at which a luminescent material returns from its excited state to the ground state, resulting in the cessation of light emission. This parameter can be directly related to the kinetics of both radiative and nonradiative transitions during the relaxation process.

The average decay lifetimes calculated for the 455 nm emission in Figure 5 from 4 might be imagined as two events due to the transition needing three exponentials to adequately fit the data between 350 and 210 K (the first event) to needing four exponentials between 190 and 77 K (the second event). This transition suggests that as the temperature is reduced, the alternative blue center decay pathway becomes viable,^[12] coinciding with our prediction of there being an additional energy state.

The first event changes from a very fast decay lifetime of 12 ms at 310 K where the 455 nm signal is very weak, to 327 ms (210 K)—30 times slower. The observed increase in the decay lifetime is supported by the data shown in Figure 6, where an alternative decay pathway could account for this effect. Such alternative pathways often involve intermediate states or energy levels in the relaxation process. These intermediate states may possess longer lifetimes or slower transition rates compared to the direct pathway of the NV⁰ center.

Furthermore, the suggested trap located between discrete energy levels could contribute to extended decay lifetimes. Traps can lead to a delayed recombination timescale for electron charge carriers confined within them however these traps could also be written in terms of holes (with additional work), primarily because of the energy cost associated with exiting the trap. This observation emphasizes that the charge carriers trapped within these states operate on a delayed timescale. It is important to note that our proposed energy diagram serves as a simplified toy model among various possibilities and assumes that the electrons and holes not involved with the trap state have already thermally equilibrated to the bottom of the band. This model is presented to facilitate a basic level of comprehension, recognizing that the entire process is intricate, and this model represents just one avenue available to be explored.

Our hypothesis is that the emergence of the hypothesized pathway is likely to occur below 150 K and is supported by the observed color change from orange to blue emission after a 90 μ s delay and at temperatures below 150 K. However, it is important to acknowledge that further investigation and experimentation are needed to fully understand and validate these proposed mechanisms.

The second event may be a result of the alternative center stabilizing within the lattice as more of the center is converted from the NV⁰ center with decreasing temperature. This is evidenced by the stark difference between the average calculated decay lifetime at 190 K (139 ms) and 210 K (327 ms). The suggestion that an alternative decay pathway may become thermally activated as the temperature is reduced is supported by the additional exponential needed to describe the data. The prospect of an alternative complex existing at lower temperatures is also supported by the calculated decay lifetime increasing linearly as the temperature is reduced to 77 K.

5. Conclusion

In this study, we have explored the above bandgap excited luminescent properties of an as-grown nitrogen-containing CVD synthetic diamond gemstone as a function of temperature using prompt and delayed photoluminescence, time-gated imaging, and temperature-dependent decay lifetime studies. We operated under the assumption that charge carriers within the diamond have already reached thermal equilibrium with the bottom of the band because their recombination timescale is significantly faster than the timescale of the unusual emission measured in this article.

Three unexpected peaks are observed in delayed photoluminescence spectra below 190 K at 419, 455, and 499 nm overlaid on a broadband emission feature centered at 465 nm. The peaks are correlated with a color change in the emission from orange to blue luminescence. Blue emission is absent in the prompt luminescence spectra but becomes observable with 90 μ s of the initial excitation. The relationship between the emission color and the time delay is further supported by the time-gated images. The observed color change suggests the possibility of an alternative decay pathway that becomes thermally activated as a function of temperature.

It is unlikely, but also cannot be ruled out, that this emission is related to the luminescence associated with dislocations, sometimes referred to as “band-A.” There have been studies on the so-called “band-A” emission using photoluminescence,^[13,14] and cathodoluminescence.^[15,16] However, previous studies have demonstrated that the above bandgap excitation of the blue dislocation luminescence in natural diamonds during the prompt timeframe is not observed from the blue luminescence observed during the delayed timeframe.^[4] The blue dislocation-like prompt luminescence observed in CVD diamond is also not observed in the delayed luminescence.^[5]

We propose the existence of an additional energy level, tentatively referred to as the “blue center”, in conjunction with a trap state within synthetic diamond gemstones. The emergence of this previously undocumented blue emission at 465 nm, accompanied by three distinct peaks, represents an intriguing discovery

in our research, which may serve as a promising addition to the exploration of synthetic diamonds.

This enigmatic blue emission, while not yet fully understood, presents an interesting reference point within the field. Our study aims to introduce this novel feature to the scientific community, thereby marking a provisional milestone in our quest for knowledge. We wish to report in the literature to signal the initial identification of this mysterious blue feature, with the hope that it may inspire future researchers to delve deeper into this intriguing area of study.

In forthcoming research, the investigation of the proposed trap state could potentially shed light on alternative decay pathways within the complex landscape of diamond energy levels, fostering a greater understanding of synthetic diamonds.

Acknowledgements

The authors extend their sincere appreciation to the research team at Element Six for generously providing the sample for our study. Furthermore, the authors acknowledge the financial support of The Engineering and Physical Sciences Research Council (Project Number: EP/W524682/1), iCase studentship, and the De Beers Group, which played a crucial role in funding and enabling this research endeavor.

Conflict of Interest

The authors declare no conflict of interest.

Data Availability Statement

The data will be available in a public repository.

Keywords

chemical vapor deposition synthetic diamonds, temperature dependence, time-gated luminescence

Received: August 30, 2023

Revised: February 5, 2024

Published online:

- [1] P. M. Martineau, S. C. Lawson, A. J. Taylor, S. J. Quinn, D. J. F. Evans, M. J. Crowder, *Gems Gemol.* **2004**, *40*, 2.
- [2] L. Tretiakova, *Eur. J. Mineral.* **2009**, *21*, 43.
- [3] S. Eaton-Magaña, C. M. Breeding, *Gems Gemol.* **2016**, *52*, 2.
- [4] C. D. McGuinness, A. M. Wassell, P. M. P. Lanigan, S. A. Lynch, *Gems Gemol.* **2020**, *56*, 2, 220.
- [5] A. M. Wassell, C. D. McGuinness, C. Hodges, P. M. P. Lanigan, D. Fisher, P. M. Martineau, M. E. Newton, S. A. Lynch, *Phys. Status Solidi A* **2018**, *215*, 1800292.
- [6] R. Guo, K. Wang, Y. Tian, H. Wang, *J. Alloys Compd.* **2022**, *924*, 166507.
- [7] Y. Xue, F. Chen, Q. Li, Z. Ju, Y. Cao, S. Zhang, X. Yuan, B. Wu, E. Wu, *Nanotechnology* **2023**, *34*, 225201.
- [8] B. Dong, C. Shi, Z. Xu, K. Wang, H. Luo, F. Sun, P. Wang, E. Wu, K. Zhang, J. Liu, Y. Song, Y. Fan, *Diamond Relat. Mater.* **2021**, *116*, 108389.
- [9] X. D. Chen, C.-H. Dong, F.-W. Sun, C.-L. Zou, J.-M. Cui, Z.-F. Han, G.-C. Guo, *Appl. Phys. Lett.* **2011**, *99*, 161903.
- [10] A. M. Zaitsev, K. S. Moe, W. Wang, *Diamond Relat. Mater.* **2018**, *88*, 237.
- [11] K. S. Moe, W. Wang, U. D'Haenens-Johansson, *Gems Gemol.* **2014**, *50*, <https://www.gia.edu/gems-gemology/summer-2014-labnotes-yellow-cvd-synthetic-diamond> (accessed: May 2023.)
- [12] L. Robledo, H. Bernien, T. Van Der Sar, R. Hanson, *New J. Phys.* **2011**, *13*, 025013.
- [13] S. Kudryashov, P. Danilov, N. Smirnov, A. Levchenko, M. Kovalev, Y. Gulina, O. Kovalchuk, A. Ionin, *Opt. Mater. Express* **2021**, *11*, 2505.
- [14] A. M. Zaitsev, *Optical Properties of Diamond*. Berlin, Springer Berlin Heidelberg, Heidelberg **2001**, <https://doi.org/10.1007/978-3-662-04548-0>.
- [15] M. Marinelli, A. Hatta, T. Ito, A. Hiraki, T. Nishino, *Appl. Phys. Lett.* **1996**, *68*, 1631.
- [16] J. Ruan, K. Kobashi, W. J. Choyke, *Appl. Phys. Lett.* **1992**, *60*, 3138.